Structure Determination of Ammonia on Cu(111)†

P. Baumgärtel, R. Lindsay, T. Giessel, O. Schaff, and A. M. Bradshaw

Fritz-Haber-Institut der Max-Planck-Gesellschaft, Faradayweg 4-6, D-14195 Berlin, Germany

D. P. Woodruff*,‡

Physics Department, University of Warwick, Coventry CV4 7AL, U.K.

Received: August 19, 1999; In Final Form: November 3, 1999

The local structure of ammonia adsorbed on Cu(111) has been determined using N 1s scanned-energy-mode photoelectron diffraction. The molecule is found to occupy an atop bonding site with a Cu−N bond length of 2.09 ± 0.03 Å, but with large amplitude vibrations of the molecule parallel to the surface, consistent with a systematic trend found in our studies of species adsorbed in atop sites. We find no evidence for a significant static offset of the molecule from the atop site (which *was* found on the lower-symmetry Cu(110) surface), but a small offset of this kind cannot be distinguished from the effects of the large dynamic displacement. As a first test for this photoelectron diffraction technique we have also investigated the effect of including the weakly scattering H atoms in the analysis. This does lead to preferred sites for the H atoms consistent with expectations, but their precision of location is too poor to provide information of chemical significance.

Introduction

There have been extensive studies of the interaction of ammonia with well-characterized surfaces, motivated especially by interest in the Haber−Bosch process which occurs over Fe catalysts, but also stemming from the potential practical importance of surface nitridation. Despite extensive spectroscopic investigations including characterization of the electronic and vibrational properties of adsorbed ammonia, there are still very few quantitative structural investigations, and while much of the structural information for ordered molecular adsorbates still derives from low-energy electron diffraction (LEED),[1] all the studies of adsorbed ammonia appear to have all been conducted by scanned-energy-mode photoelectron diffraction (PhD).[2] Investigations of ammonia adsorbed on Ni(111)[3] and Ni(100)[4] by this method have both led to the conclusion that the molecule adsorbs atop a surface layer Ni atom in a symmetric position, although in the case of Ni(111), at least, the molecule appears to undergo a large-amplitude frustrated translational mode parallel to the surface. More recently the same approach has been applied to ammonia adsorbed on Cu(110),[5] and while the bonding is also found to be atop, the local geometry was found to be of low symmetry with a significant off-atop location; this surprising result seems to be supported by an independent ESDIAD (electron-stimulated desorption ion angular distribution) investigation.[6]

In this paper we present the results of a similar study of ammonia adsorbed on Cu(111), but including an investigation of the role of the weakly scattering H atoms with a view to exploring the ability of the PhD technique to provide a complete structural solution for this adsorbate. Total energy calculations suggest that an atop geometry is also to be expected on this surface.[7,8] There have been a number of nonstructural studies of this adsorption system, although many of these have concentrated on its novel photodesorption characteristics.[9−14] Here we concentrate not on these dynamical aspects, but on the local equilibrium structure.

Experimental Details and Results

The experiments described here were performed in a purpose-built UHV chamber on the HE-TGM-1 monochromator at the Berlin synchrotron radiation source BESSY.[15] The scanned-energy-mode photoelectron diffraction technique[2] is based on the analysis of the intensity modulation of the photoemission signal from an adsorbate core level in specific directions as a function of photoelectron kinetic energy. The interference of the directly emitted component of the photoelectron wave field with other components elastically scattered by atoms surrounding the emitter leads to these modulations, which are dependent on the scattering-path-length differences. These modulations can thus be related to the local structural environment of the emitter. The photoelectron diffraction data were collected using a 150° spherical-sector electron analyzer (of mean radius 152 mm) mounted at a fixed angle of 60° relative to the photon incidence direction and fitted with three parallel channeltrons (VG Scientific). To obtain the required N 1s PhD spectra, short (60 eV) electron energy spectra were recorded around the N 1s peak at photon energies separated by 2 eV increments in the energy range 450−870 eV. Each of these was then fitted by an appropriate peak and background, and the resulting peak areas were then plotted as a function of the photoelectron peak energy; a smooth spline fit to this plot was then subtracted and divided into the intensities to produce properly normalized PhD modulation spectra.[2] N 1s PhD spectra of this type were obtained at polar emission angles between 0° and 60° in steps of 10° in each of the three principal azimuths, [1$\bar{2}$1], [1$\bar{1}$1], and [2$\bar{1}\bar{1}$] (equivalent to [$\bar{1}$21]). A subset of nine of these spectra (see Figure 1), representative of a range of emission directions (but centered around normal emission where the strongest modulations are seen), was used in the subsequent structural analysis.

* To whom correspondence should be addressed. E-mail: D.P.Woodruff@Warwick.ac.uk. Fax: +44 1203 692016.

† Part of the special issue "Gabor Somorjai Festschrift".

‡ Also at the Fritz-Haber-Institut der Max-Planck-Gesellschaft.

10.1021/jp992925a CCC: $19.00
Published on Web 12/30/1999

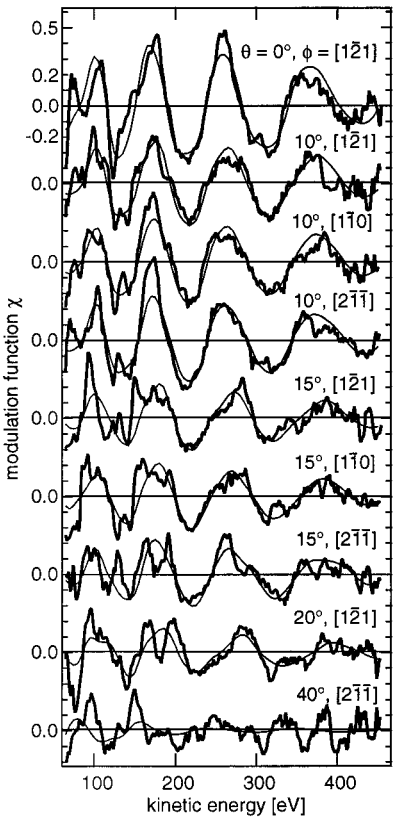

Figure 1. Experimental (bold lines) N 1s PhD spectra recorded from NH_3 adsorption on Cu(111). The thin lines show the results of simulations for the best-fit symmetric atop structure described in the text. The convention for the definition of the ⟨112⟩ azimuthal directions relative to the structure of Cu(111) is defined in Figure 3, which shows the [$\bar{1}2\bar{1}$] direction (which is equivalent to [2$\bar{1}\bar{1}$] and opposite [1$\bar{2}$1]).

The Cu(111) crystal was prepared by the usual combination of X-ray Laue alignment, spark machining, mechanical polishing, and electropolishing, followed by in situ Ar^+ bombardment and annealing cycles, the cleanness being verified by soft X-ray (core-level) photoelectron spectroscopy (SXPS) using the synchrotron radiation as the radiation source. The LEED (low-energy electron diffraction) pattern revealed a sharp (1×1) surface net expected for a well-ordered clean surface. Experiments on the ammonia adsorbate concentrated on the medium-coverage (β_1[9]) phase which was prepared by exposing the sample at 130 K to 4×10^{-6} mbar·s of NH_3 gas. The previous thermal desorption characterization of this phase indicates a coverage of 0.1 monolayer (ML); on the basis of a comparison of SXPS spectra from the nominal 0.5 ML Cu(100)c$(2 \times 2)-$N phase we estimate a coverage of 0.12 ± 0.012 ML. In view of the interest in the photodesorption properties of this system, we should add that we saw no evidence of any significant influence of the monochromatic synchrotron radiation beam on our sample during the course of the measurements. Tests using zero-order light, however, did show strong beam-induced effects in the N 1s photoemission peak intensity and line shape, indicating some conversion to a new species, possibly accompanied by some photodesorption.

Structure Analysis

Our methodology for structure determination using PhD comprises two steps. First, we apply a direct inversion of the experimental spectra using the so-called projection method[16,17] which gives an "image" of the location of the (substrate) scattering atoms surrounding the adsorption site together with an approximate value for the nearest-neighbor bond length. The projection method exploits the fact that PhD spectra recorded in emission directions which have a near-neighbor substrate scatterer directly behind the emitter are typically dominated by the interference from this single scattering path, in part due to the peaking of the backscattering cross-section around 180° scattering. If one therefore calculates the amplitude of the projection integral of the experimental spectra onto simulated spectra for single scattering from a substrate atom at each possible location in three-dimensional space, this will peak when the amplitude and phase of theory match those of a large component of the experimental spectra. The locations of the dominant peaks in the projection integrals can provide valuable approximate information on the likely locations of substrate near-neighbors to the emitter and thus the local structure.

This approximate structure from the projection method is used as a starting model in the second step which consists of the simulation of the experimentally determined modulation functions using multiple scattering calculations. These calculations are performed with computational codes developed by Fritzsche, which use an expansion of the scattering processes into scattering paths.[18,19] The successive scattering events on a scattering path are treated within a Green's function formalism using a magnetic quantum number expansion for the free electron propagator.[20] The quality of agreement between the simulated modulation functions compared with the corresponding experimental spectra is quantified using a reliability factor (R factor), normalized such that its value is zero for complete agreement between theory and experiment, unity for no correlation between theory and experiment, and two for anticorrelation.[3] To optimize the efficiency of the search of structural parameter space to find the structure corresponding to the best agreement, we use an adapted Newton−Gauss algorithm and an approximate "linear" version of the multiple scattering code in the initial searches.[18,21] The precision of the final structural parameters and the significance of any improved fit to the data are estimated with the aid of a variance for the minimum value of the R factor, R_{min}, defined in a way similar to Pendry's suggestion for a similar parameter in LEED structure determinations[22] as described by us in more detail elsewhere.[23] Any structure which is found to have an associated R factor less than $R_{min} + \mathrm{var}(R_{min})$ is regarded as falling within the error limits. Notice that the standard approach to defining errors in this way is to investigate the dependence of the R factor on each individual structural parameter, a method which neglects the possible influence of coupling of structural parameters (when an increase in the R factor by changing one parameter can be offset by a change in another parameter). In the present case we have checked for such coupling and given worst-case error estimates which take account of this effect. The most significant example of this coupling is discussed in detail below.

Figure 2 shows the results of applying the first stage of this procedure, the direct inversion "projection method", to the experimental N 1s PhD modulation spectra from NH_3 adsorbed on Cu(111). This calculation leads to a parameter which depends on the position in three-dimensional space around the emitter, the magnitude of which is related to the probability of finding a backscatterer atom at any position. In Figure 2 a gray-scale mapping of this parameter is shown in two different two-dimensional sections through this space. The upper panel shows a plane perpendicular to the surface in a ⟨112⟩ azimuth with the emitter at (0,0,0). The only intensity visible is a dish-shaped feature approximately 2.1 Å directly below the emitter; the shape of this feature reflects, in part, the fact that the projection method

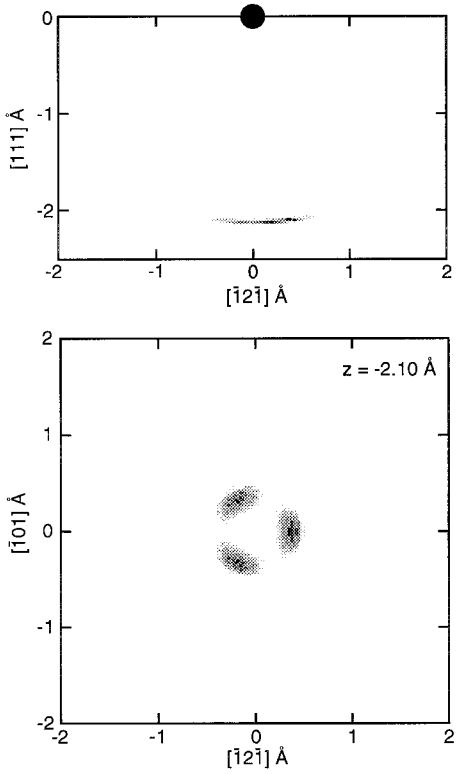

Figure 2. Gray-scale map sections perpendicular to the surface in a ⟨112⟩ azimuth (top) and parallel to the surface but 2.10 Å below the N emitter (at (0,0,0)) (bottom) showing the results of the application of the projection method of direct data inversion to the experimental N 1s PhD spectra as shown in Figure 1.

maps the intersections of contours of constant scattering-path-length difference which are paraboloids. Clearly, however, this result indicates that a Cu backscatterer lies approximately directly below the N emitter, consistent with occupation of an atop site. The lower panel of Figure 2 shows a section parallel to the surface 2.10 Å below the emitter and thus cutting through this dish-shaped feature. We see that it actually comprises three peaks offset in the three equivalent [$\bar{1}2\bar{1}$] azimuths by approximately 0.3 Å. This could be reconciled with the N atom occupying sites displaced by this amount from atop, indicating a tilt of the Cu−N bond relative to the surface normal of about 9°. The preliminary conclusion from this direct data inversion, therefore, is that the ammonia is bonded close to atop a surface Cu atom, but probably has some small tilt of the Cu−N bond toward an fcc hollow site (i.e., the hollow site which lies directly above a third-layer Cu atom in the substrate). This structural model is shown schematically in Figure 3 in which the azimuthal definitions are also shown; notice in particular that the fact that the Cu nearest-neighbors appear to offset in the [$\bar{1}2\bar{1}$] direction means that the N emitter must be offset from atop in the opposite ([$1\bar{2}1$]) direction.

Although this first-order structural information does indicate some slight offset from the ideal atop geometry, our detailed optimization of the structure using the multiple scattering simulations started first from the more symmetric ideal atop site. In all of these calculations, as has been common for our earlier PhD studies and quantitative LEED investigations of molecular adsorption geometries, the H atoms (which are very weak scatterers) were not included in the calculations. Placing the N emitter directly 2.10 Å atop a surface Cu atom of a bulk-terminated Cu(111) surface, assuming all mean-square vibrational amplitudes to be 0.003 Å^2 (as implied for the bulk from the known Debye temperature), yielded an *R* factor value of

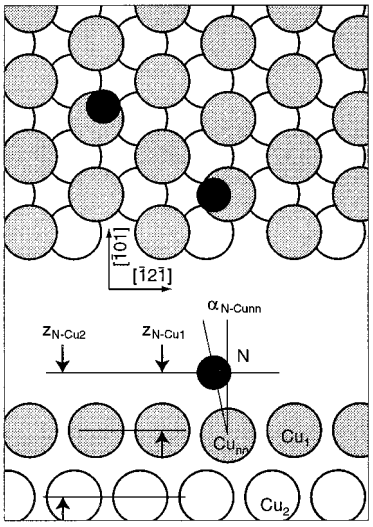

Figure 3. Schematic plan (top) and sectional (bottom) views of the local N adsorption site in NH_3 adsorbed on Cu(111) inferred from the results of Figure 2. The main structural parameters investigated in the multiple scattering simulations are defined in this diagram, as are two of the azimuthal directions which determine the convention for labeling the ⟨112⟩ azimuths.

0.28 for the set of nine PhD spectra used in the analysis. This value already represents a reasonable fit on the basis of previous, similar analyses with PhD.

The next stage of optimization of the structure involved allowing adjustment of the local Cu−N and Cu−Cu layer spacings around the adsorbed NH_3 molecule as well as the vibrational amplitudes, nevertheless retaining the symmetric atop site. In particular, the layer spacing of the N atom relative to the nearest neighbor surface Cu atom, z_{N-Cunn}, to the remainder of the top-layer Cu atoms, z_{N-Cu1}, and to the second Cu atom layer, z_{N-Cu2}, were varied. In addition, the mean-square vibrational amplitude of all the Cu atoms other than the nearest-neighbor were allowed to vary, while the mean-square vibrational amplitude of the nearest-neighbor Cu atom was allowed to take a different value, and the N emitter itself was allowed to take different vibrational amplitudes parallel and perpendicular to the surface. The resulting fit gave a low *R* factor of 0.16 and the very good fit shown in Figure 1. The resulting structural parameter values were $z_{N-Cunn} = 2.09 \pm 0.03$ Å, $z_{N-Cu1} = 2.02 \pm 0.40$ Å, and $z_{N-Cu2} = 4.22 \pm 0.17$ Å.

Notice that in the PhD technique the key structural parameters are all relative to the emitter location; moreover, in the present case in which only near-normal emission spectra show strong modulations (see below), the data are rather insensitive to the positions of scatterers which lie in directions far from the surface normal relative to the emitter. Thus, the data are very sensitive to the location of the nearest-neighbor Cu atom but show almost no sensitivity to the location of the other top-layer atoms. The underlying reason for this weak off-normal modulation of the spectra is directly related to the very large vibrational amplitude parallel to the surface (see Table 1), which suppresses the importance of scattering paths containing a significant vector component parallel to the surface through its associated Debye−Waller factor. This effect was first remarked upon in our much earlier study of NH_3 adsorption on Ni(111).[24] We should note, however, that proper interpretation of the physical significance of the fitted vibrational amplitudes requires some care. In the case of uncorrelated vibrations the relative mean-square vibrational amplitude of two atoms is simply the sum of their respective mean-square vibrational amplitudes. This situation

TABLE 1: Values of the Vibrational Fitting Parameters Obtained for the Symmetric Atop Geometry and the Inferred "True" Values As Described in the Text[a]

vibration	fitting value (Å^2)	true value (Å^2)
$\langle u^2_{\mathrm{N(parallel)}}\rangle$	0.075(−0.060/+0.190)	0.079(−0.061/+0.230)
$\langle u^2_{\mathrm{N(perpendicular)}}\rangle$	0.0018(−0.0018/+0.0020)	0.0056(−0.0056/+0.1300)
$\langle u^2_{\mathrm{Cunn}}\rangle$	0.0024(±0.0020)	0.077(−0.060/+0.190): parallel and relative 0.0042(−0.027/+0.0028): perpendicular and relative
$\langle u^2_{\mathrm{Cu}}\rangle$	0.0068(−0.0068/+0.1300)	0.0030 (fixed)

[a] Note that the inferred vibrational amplitudes for the Cunn (nearest neighbor Cu) atom are relative to the N emitter and not true absolute vibrational amplitudes.

is expected to be relevant to the vibrations of the emitter relative to most of the Cu substrate atoms. On the other hand, we can expect the nearest-neighbor Cu atom to the N emitter to show some correlation in its vibrations, so this simple connection to the true uncorrelated vibrations is lost. In many adsorbate systems the true vibrational amplitude of the adsorbate (as in the present case parallel to the surface) can be very much larger than those of the bulk atoms, but also larger than the relative vibrational amplitude of the correlated nearest-neighbors. To simulate this effect, it is helpful to allow the bulk vibrational amplitudes to increase beyond their true values, such that the apparent emitter vibrational amplitude falls sufficiently for true correlated near-neighbor values to be incorporated. Of course, the true bulk atom vibrational parameters can be estimated quite easily from the known Debye temperature, so imposing this value allows one to redistribute the vibrational parameters obtained in the fits to their physically meaningful locations. Table 1 shows both the actual fitting parameters and inferred "true" vibrational parameters, assuming a bulk mean-square vibrational amplitude of 0.003 Å^2.

The very large optimum value of the vibrational amplitude of the N emitter parallel to the surface (the mean-square vibrational amplitude of 0.079 Å^2 corresponds to a root-mean-square value of 0.28 Å) is broadly consistent with the idea that an atop-bonded adsorbate can have a very soft frustrated translational mode parallel to the surface which may therefore be readily excited to large amplitude. As remarked above, we first noticed this effect for NH_3 adsorption on Ni(111), but have also seen it in other molecular and atomic adsorption systems involving atop geometries such as PF_3 on Ni(111),[25] CO on Cu(110),[26] and K on Ni(111).[27] Of course, we should also stress that the precision of the actual size of this vibrational amplitude in the present case is very poor (see Table 1), but even the smallest value acceptable is anomalously large relative to the bulk vibrational amplitudes.

So far we have concentrated on the fully symmetric atop adsorption geometry despite the fact that the direct inversion "image" of Figure 2 suggests a local displacement from this site. In considering possible reoptimizations of the structural fit to include a possible offset, we have tested four different models, shown schematically in Figure 4. In models (a) and (b) it is assumed that the displacements are toward either the fcc or hcp hollow sites, respectively ((a) being the model implied by Figure 2). In (c) both displacements are considered equally probable, while in (d) the displacement is assumed to be in the intermediate ⟨110⟩ azimuth, in this case also assuming the offset reflected the local (top-layer) 6-fold symmetry. Tests actually showed that all of these models yielded the same optimum tilt angle of the Cu−N bond, α, of 5 ± 5°, while the value of the optimum value of the fitting parameter $\langle u^2_{\mathrm{N(parallel)}}\rangle$ fell slightly to 0.05(−0.05/+0.21) Å^2. The *R* factor value for all of these fits was identical, to three significant figures (0.162), to the value obtained for the symmetric atop site described above. This behavior is consistent with previous studies (e.g., of NH on Cu-

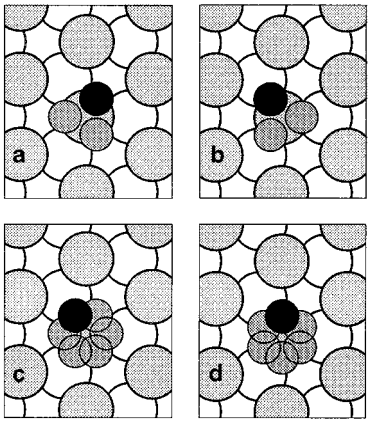

Figure 4. Schematic plan view of four possible models involving NH_3 adsorption offset from the ideal atop site. In each model the bold small circle shows one off-atop N atom location, while the other more lightly shaped small circles show the other sites considered equally possible. The large circles represent the top-layer (shaded) and second-layer (open) Cu atoms.

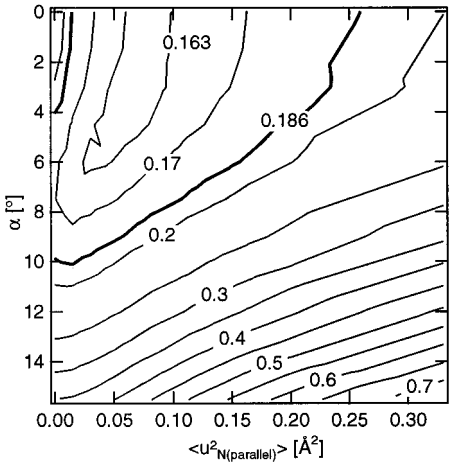

Figure 5. Contour map of the dependence of the *R* factor quantifying the experiment/theory fit on the static offset of the NH_3 molecule from atop, determined by the Cu−N bond angle, α, and the mean-square vibrational amplitude of the N emitter atom parallel to the surface. The bold contour defines the limits of acceptable solutions corresponding to an *R* factor value equal to the sum of the minimum value (0.162) and the variance (0.024).

(110)[28]) in which there is a strong correlation between a static offset parameter (of small magnitude) and a dynamic vibrational amplitude in the same direction. This correlation is illustrated in Figure 5, which shows a contour map of the *R* factor value as a function of these two parameters. Notice the markedly diagonal character of the contour lines which characterizes such parameter coupling. The result is entirely consistent with the basic physics of the PhD process; static offsets from symmetric locations require domain averages over all symmetry-equivalent offsets, and leads to dephasing of the scattering paths in a

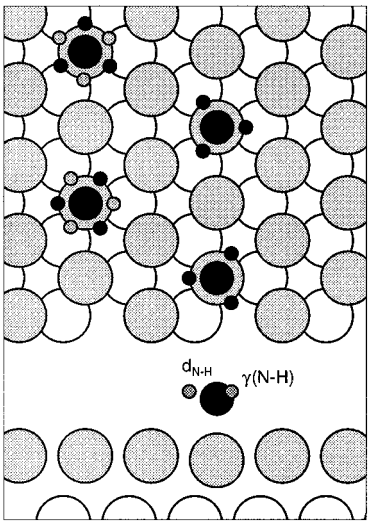

Figure 6. Plan (top) and section (bottom) view of the models tested to determine the H atom locations for NH_3 adsorbed atop on Cu(111), together with the definition of the associated structural parameters.

fashion very similar to that produced by the Gaussian distribution of positions implicit in the treatment of vibrational disorder. It is unclear whether the apparent offset seen in the projection method is a direct consequence of the same effect or an artifact of the method.

As a final test of the PhD method in this system, we have also explored the influence of the H atoms in the adsorbed ammonia and the possibility of obtaining some information on their location. The key structural fitting parameters in adding the H atoms are the N−H bond length, d_{N-H}, and the angle of this bond relative to the surface normal (and the symmetry axis of the molecule for the ideal atop site), γ_{N-H}. In addition, of course, one must establish the influence of different possible azimuthal orientations of the N−H bonds, and both individual and mixed orientation models, as shown schematically in Figure 6, were tested, while the vibrational amplitude of the H atom was also optimized. For these tests the molecule was constrained to occupy the symmetric atop site again. This new optimization did lead to an improvement in the overall *R* factor (ultimately from 0.162 to 0.151), although the improvement is not formally statistically significant in that it is less than the variance (0.022). This improvement was not sensitive to the azimuthal orientational model used, and indicated a preference for essentially no vibration of the H atom (but with an estimated precision in the mean-square vibrational amplitude of ±0.02 Å^2). The optimum value of d_{N-H} was 1.0(−0.05/+1.0) Å and of γ_{N-H} was 75(−15/+45)°. Both of these clearly show poor precision but do encompass expected values (for the free ammonia molecule these values are 1.12 Å and 68°). This best fit also involved some reduction of the optimum value of the mean-square vibrational amplitude of the N atom parallel to the surface from 0.075 to 0.045 Å^2, a value similar to that obtained when the molecule was allowed to tilt, but also well within the error estimates of all the models. Notice that although the improvement in the *R* factor produced by the inclusion of the H atoms in this geometry is such that the model without H atoms falls within the variance, one can define a precision for the H atom locations because moving them far from the optimum positions does lead to an increase in the *R* factor outside the variance. This is shown in Figure 7, which shows the basis of these precision estimates. In view of the fact that we know the H atoms *are* present, it is therefore interesting to note that we do find their preferred locations to be consistent with expectations.

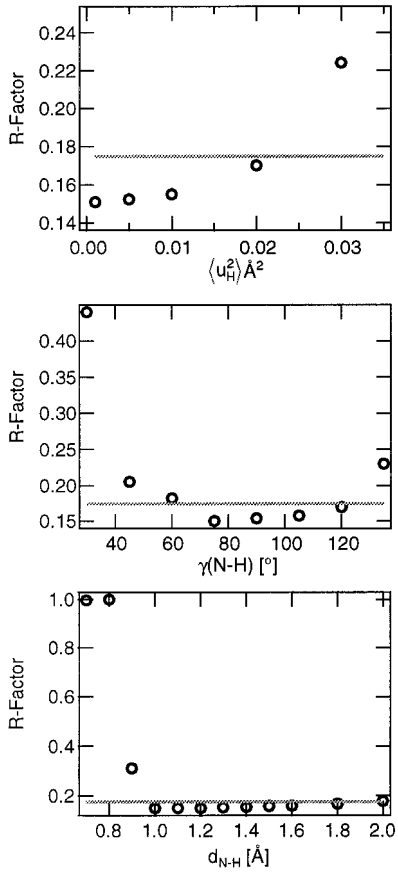

Figure 7. Dependence of the *R* factor on the structural parameters associated with the H atoms. The horizontal lines in each case correspond to a value of the *R* factor equal to the sum of its minimum value and its variance, and thus define the limits of acceptable solutions.

On the other hand, the poor precision in locating these weak scatterers means that we have learned nothing of real significance about the structure from this exercise.

Conclusions

Our detailed quantitative analysis of the adsorption geometry of NH_3 on Cu(111) confirms the predictions of theoretical calculations and the general trend of earlier experimental studies on Ni(111) and Ni(100) that the molecule adopts an atop site. We also find evidence for large-amplitude vibrations of the molecule parallel to the surface, a systematic trend of many of our studies of species adsorbed in atop sites. We find no evidence for a significant static offset of the molecule from the atop site (which *was* found on the lower-symmetry Cu(110) surface), but a small offset of this kind cannot be distinguished from the effects of the large dynamic displacement. The Cu−N bond length found in this adsorption system is 2.09 ± 0.03 Å, consistent with the value found on Cu(110) of 2.04 ± 0.03 Å. This value is significantly longer than the Ni−N bond length found for ammonia adsorption on Ni(111) of 1.97 ± 0.03 Å or even the value of 2.01 Å found on Ni(100); these comparisons suggest that there is a significant difference in the local bond length on Cu and Ni (which have almost identical metallic radii), which is presumably attributable to a difference in bonding strength. We have also demonstrated that the photoelectron diffraction technique does show some sensitivity to the location of the H atoms despite their weak scattering, although the precision in locating these atoms is insufficient to provide any further insight into the adsorbate−substrate bonding.

Acknowledgment. This work was supported by the German Federal Ministry of Education, Science, Research and Technology (Contract No. 05 625EBA 6), by the European Community HCM program through Large Scale Facilities support to BESSY, and by the Physical Sciences and Engineering Research Council (U.K.) in the form of a research grant and a Senior Research Fellowship for D.P.W. A.M.B. and D.P.W. also thank the Max-Planck-Gesellschaft and the Alexander-von-Humbolt-Stiftung for a Max-Planck-Research Prize. We thank Volker Fritzsche for providing the multiple scattering codes.

References and Notes

(1) Van Hove, M. A.; Somorjai, G. A. *J. Mol. Catal., A* **1998**, *131*, 243.
(2) Woodruff, D. P.; Bradshaw, A. M. *Rep. Prog. Phys.* **1994**, *57*, 1029.
(3) Schindler, K.-M.; Fritzsche, V.; Asensio, M. C.; Gardner, P.; Ricken, D. E.; Robinson, A. W.; Bradshaw, A. M.; Woodruff, D. P.; Conesa, J. C.; Gonzalez-Elipe, A. R. *Phys. Rev. B* **1992**, *46*, 4836.
(4) Zheng, Y.; Moler, E.; Hudson, E.; Hussain, Z.; Shirley, D. A. *Phys. Rev. B* **1993**, *48*, 4760.
(5) Booth, N. A.; Davis, R.; Toomes, R. L.; Woodruff, D. P.; Hirschmugl, C.; Schindler, K.-M.; Schaff, O.; Fernandez, V.; Theobald, A.; Hofmann, Ph.; Lindsay, R.; Giessel, T.; Baumgärtel, P.; Bradshaw, A. M. *Surf. Sci.* **1997**, *387*, 152.
(6) Mocuta, D.; Ahner, J.; Yates, J. T., Jr. *Surf. Sci.* **1997**, *383*, 299.
(7) Bagus, P. S.; Hermann, K.; Bauschlicher, C. W., Jr. *J. Chem. Phys.* **1984**, *81*, 1966.
(8) Biemolt, W.; van de Kerkhof, G. J. C. S.; Davies, P. R.; Jansen, A. P. J.; van Santen, R. A. *Chem. Phys. Lett.* **1992**, *188*, 477.
(9) Hertel, T.; Wolf, M.; Ertl, G. *J. Chem. Phys.* **1995**, *102*, 3414.
(10) Saalfrank, P.; Holloway, S.; Darling, G. R. *J. Chem. Phys.* **1995**, *103*, 6720.
(11) Guo, H.; Seideman, T. *J. Chem. Phys.* **1995**, *103*, 9062.
(12) Hertel, T.; Wolf, M.; Ertl, G. *Chem. Phys. Lett.* **1996**, *257*, 155.
(13) Hasselbrink, E.; Wolf, M.; Holloway, S.; Saalfrank, P. *Surf. Sci.* **1996**, *363*, 179.
(14) Torri, M.; Gortel, Z. W.; Teshima, R. *Phys. Rev. B* **1998**, *58*, 13982.
(15) Dietz, E.; Braun, W.; Bradshaw, A. M.; Johnson, R. L. *Nucl. Instrum. Methods, A* **1985**, *239*, 359.
(16) Hofmann, Ph.; Schindler, K.-M. *Phys. Rev. B* **1993**, *47*, 13941.
(17) Hofmann, Ph.; Schindler, K.-M.; Bao, S.; Bradshaw, A. M.; Woodruff, D. P. *Nature* **1994**, *368*, 131.
(18) Fritzsche, V. *Surf. Sci.* **1989**, *213*, 648.
(19) Fritzsche, V. *J. Phys.: Condens. Matter* **1990**, *2*, 1413.
(20) Fritzsche, V. *Surf. Sci.* **1992**, *265*, 187.
(21) Fritzsche, V.; Pendry, J. B. *Phys. Rev. B* **1993**, *48*, 9054.
(22) Pendry, J. B. *J. Phys. C* **1980**, *12*, 937.
(23) Booth, N. A.; Davis, R.; Toomes, R. L.; Woodruff, D. P.; Hirschmugl, C.; Schindler, K.-M.; Schaff, O.; Fernandez, V.; Theobald, A.; Hofmann, Ph.; Lindsay, R.; Giessel, T.; Baumgärtel, P.; Bradshaw, A. M. *Surf. Sci.* **1997**, *387*, 152.
(24) Fritzsche, V.; Schindler, K.-M.; Gardner, P.; Bradshaw, A. M.; Asensio, M. C.; Woodruff, D. P. *Surf. Sci.* **1992**, *269*/*270*, 35.
(25) Dippel, R.; Weiss, K.-U.; Schindler, K.-M.; Gardner, P.; Fritzsche, V.; Bradshaw, A. M.; Asensio, M. C.; Hu, X. M.; Woodruff, D. P.; González-Elipe, A. R. *Chem. Phys. Lett.* **1992**, *199*, 625.
(26) Hofmann, Ph.; Schindler, K.-M.; Bao, S.; Fritzsche, V.; Bradshaw, A. M.; Woodruff, D. P. *Surf. Sci.* **1995**, *337*, 169.
(27) Davis, R.; Hu, X. M.; Woodruff, D. P.; Weiss, K.-U.; Dippel, R.; Schindler, K.-M.; Hofmann, Ph.; Fritzsche, V.; Bradshaw, A. M. *Surf. Sci.* **1994**, *307*−*309*, 632.
(28) Hirschmugl, C.; Schindler, K.-M.; Schaff, O.; Fernandez, V.; Theobald, A.; Hofmann, Ph.; Bradshaw, A. M.; Booth, N. A.; Davis, R.; Woodruff, D. P.; Fritzsche, V. *Surf. Sci.* **1996**, *352*−*354*, 232.